Project report

by Mubin N Group

POWER GENERATION USING RECTENNA

Submitted in partial fulfillment of the requirements

of the degree of

Bachelor of Engineering

in

Electronics and Telecommunication

by

MOHD MUBEEN(16DET95)
KHAN ASAD(16DET91)
ALAM MEHRAB(16DET73)
QURESHI SAMEER(16DET114)

Under the guidance of

PROF (RAHUL KHADSE)

Department of Electronics and Telecommunication Engineering

Anjuman-I-Islam's Kalsekar Technical Campus
Sector 16, New Panvel , Navi Mumbai
University of Mumbai

2020-21

CERTIFICATE

Department of Electronics and Telecommunication Engineering
Anjuman-I-Islam's Kalsekar Technical Campus
Sector 16, New Panvel , Navi Mumbai
University of Mumbai

This is to certify that the project entitled **POWER GENERATION USING RECTEENA** is a bonafide work of **MOHD MUBEEN(16DET95), KHAN ASAD(16DET91),ALAM MEHRAB(16DET73), QURESHI SAMEER(16DET114)** submitted to the University of Mumbai in partial fulfillment of the requirement for the award of the degree of Bachelor of Engineering in Department of Electronics and Telecommunication Engineering.

Supervisor

Examiner

Head of Department

Director

Project Report Approval for Bachelor of Engineering

This project entitled "**POWER GENERATION USING RECTENNA**" by **MUBEEM,ASAD,MEHRAB,SAMEER** is approved for the degree of **Bachelor of Engineeringin Electronics and Telecommunication** .

Examiner

.....

Supervisor

.....

Date;

Place:

Declaration

I declare that this written submission represents my ideas in my own words and where others ideas or words have been included, I have adequately cited and referenced the original sources. I also declare that I have adhered to all principles of academic honesty and integrity and have not misrepresented or fabricated or falsified any idea/data/fact/source in my submission. I understand that any violation of the above will be cause for disciplinary action by the Institute and can also evoke penal action from the sources which have thus not been properly cited or from whom proper permission has not been taken when needed.

.....
MOHAMMAD MUBEEN
(16DET95)

.....
KHAN ASAD
(16DET91)

.....
ALAM MEHRAB
(16DET73)

.....
QURESHI SAMEER
(16DET114)

Date:

Acknowledgments

We have taken efforts in this project. However, it would not have been possible without the kind support and help of many individuals . I would like to extend my sincere thanks to all of them.

We am highly indebted to (PROF RAHUL KHADSE) for their guidance and constant supervision as well as for providing necessary information regarding the project & also for their support in completing the project.

We would like to express my gratitude towards my parents & Staff of Anjuman-I-Islam's Kalsekar Technical Campus for their kind co-operation and encouragement which help me in completion of this project.

.

We My thanks and appreciations also go to my colleague in developing the project and people who have willingly helped me out with their abilities.

MOHAMMAD MUBEEN(16DET95)
KHAN ASAD(16DET91)
ALAM MEHRAB(16DET73)
QURESHI SAMEER(16DET114)

Appendix I **7**

Content

Abstract

With the rapid development of wireless systems and the demands of low-power electrical circuits, various research methods often study the feasibility of installing these circuits by harvesting free energy in a power supply or using a dedicated RF source. Wireless transmission technology (WPT) was first adopted by Tesla a hundred years ago. However, it has faced several challenges of deploying actual applications. Recently, energy harvesting technology and WPT technology have received a lot of attention as a clean and renewable energy source. The Rectenna (rectifying antenna) system can be used to remotely charge over multiple sensor networks online of app objects as they are widely used in smart devices, installed medical devices and automotive applications. The Rectenna, which is used to convert from RF power to DC power, is mainly a combination between an acquired antenna and a redirect circuit. This chapter will introduce a number of single and multiband rectennas with various features of energy harvesting applications. One-to-one multiband horns and repair circuits with similar networks are included in the fully-fledged circuit models. At the end of the chapter, a model with a double-band rectenna is presented with a detailed description of each part of the rectenna.

Highlights: Dedicated RF source, directional radiation pattern, highly beneficial antenna, rectenna (adjusting antenna), RF power harvest, wireless power transfer (WPT)

Chapter 1

1. Introduction

Wireless power transmission (WPT) can be divided into three distinct categories as shown in Figure 1: a potential field adjacent field,
empowered to command a distant field, and to harvest the most distant field of fields. In the first stage, usually occurs between two coils, one is primary and the other is secondary. The main purpose is to transfer power from the main coil to the second coil by several inches as a distance between them [1-3]. Many proposed DGS projects (DGS) are proposed for this type of wireless power transfer [4-6] to provide optimal system efficiency.

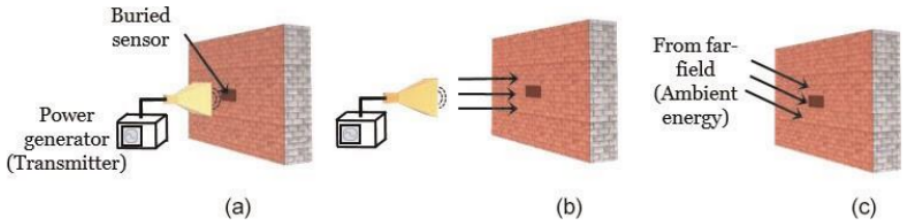

Figure 1.
The WPT categories are (a) strong adhesion or metal welding near, (b) remote field empowerment and (c) remote wireless power harvesting.

The second stage of the WPT is a long-distance demonstration power that is used by transmitting command power which means that the transfer takes place in the most remote area but with a well-defined source direction. This type of WPT is useful for solar power applications (SPS) [7-9] or by deliberately installing power such as using a supply source with a well-known direction to power the wireless sensor network, each sensor has a built-in rectenna used as a renewable energy source to power the connected sensor . The third type is to harvest the power of a distant field. The recipient does not know what the direction of the received power is. Therefore, one of the main objectives of this model is to increase the chances of acceptance by designing antennas with a wide range of frequency and maximum resonance frequency. WPT near the field provides short-term power solution for electronic devices, becoming widely marketed in many wireless applications [10 - 12]. Nearby field transfers can also help with wireless devices [13 - 13]. However, nearby field WPT has a major problem with regard to transmission distance, covering very short distances (a few inches); therefore this reduces its use. On the other hand, a dedicated remote source power system or free stand-alone power system may be able to overcome this problem due to long-distance charging capacity. Several studies have been presented in the wireless power harvest [16 - 25]. Although, with a strong focus on wireless energy harvesting, there are many obstacles in the way of harvesting free energy sources. One of the major drawbacks is the low ambient power input rates. As a result, there are many research papers presented by recteners at low levels of electrical input. However, single-band rectennas have simpler structures, many research studies [26 - 31] have investigated multi-band rectennas as an attempt to increase the split strength obtained with the same rectenna device; introduced various individual and multiple rectennas. Also, there are significant challenges with regard to the performance of the rectenna in terms of constant volatility values in the range of signal obtained. Therefore, Section 2 introduces the literature study on the performance of the single and plural frequency of different rectena; also, various designs of rectennas that operate with lower input and higher in diameter are discussed. Finally, in Section 3, a dual-band rectenna using a voltage doubler receiver and a four-phase network is discussed as an example of the performance of two bands to show the various stages of the entire rectenna system in detail. A two-band antenna is, first, designed, built and measured separately to test antenna performance. After that, the rectifier with the same network between the antenna and the repair circuit is also designed and tested independently. Thereafter a coupling between the antenna and the rectifier was performed on the same PCB substrate.

Chapter 2

2. Literature review

5 Low input received power rectennas

In [32], a compact dual-band rectenna is proposed as depicted in Figure 2. The rectenna has a conversion efficiency of 38 and 31% at 900 MHz and at 4.45 GHz,

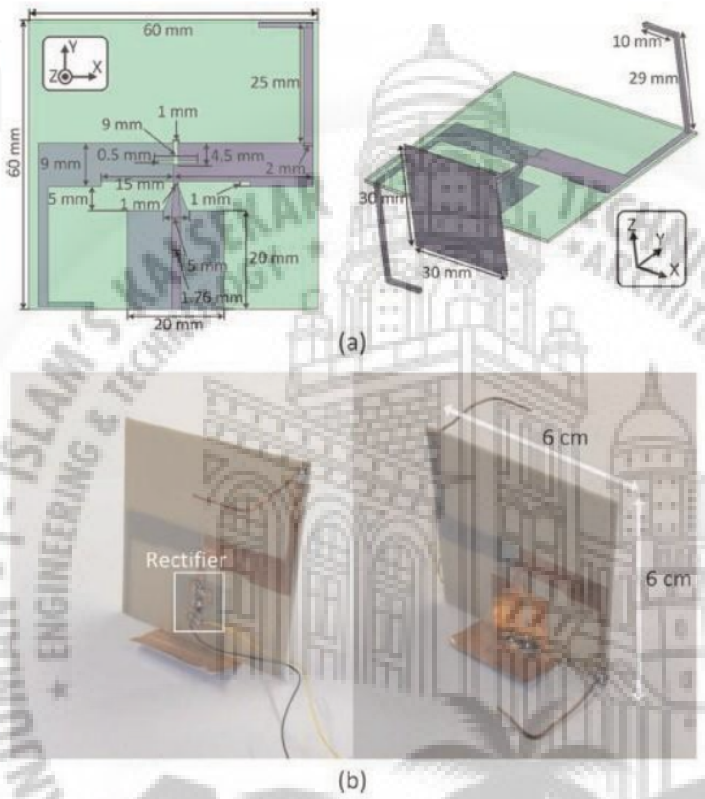

Figure 2.
Rectenna design: (a) design of the top and side view and (b) fabricated rectenna prototype [32].

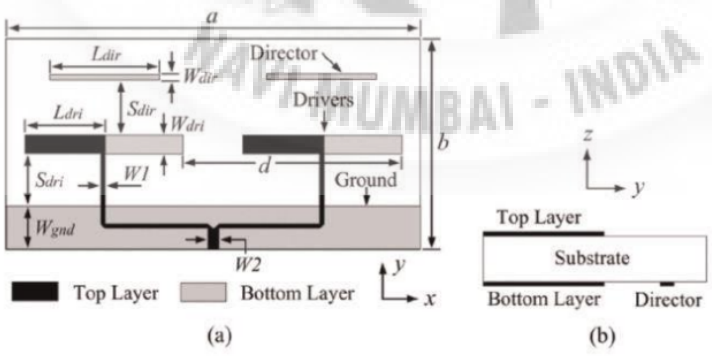

Figure 3.
Layout of the quasi-Yagi subarray. (a) Top view. (b) Side view [33].

3

respectively, with an input power of 10 dBm and a resistance load of 22.1 kΩ. Dual-band
In this region we are talking about the circle with different wavelengths in the rectenna and yagi uda antenna
1d their frequency measurements
rectenna using Yagi antenna for low power in1t applications shown in Figure 3 introduced in [33] GHz with an input power of 10 dBm. The link between solar energy and RF energy harvesting is discussed in [34]. This solar rectenna, shown in Figure 4, achieves 15% RF-DC performance conversion with a input power of -25dBm at 990 MHz and
2.45 GHz. At [35], the 130 nm PMOS rectifier is proposed for ultra-low input power. Figure 5 shows th2 structure of the rectenna. It consists of 10 stages of providing maximum performance of 45.86% in -19 dBm input power and DC voltage of 4.36 V in

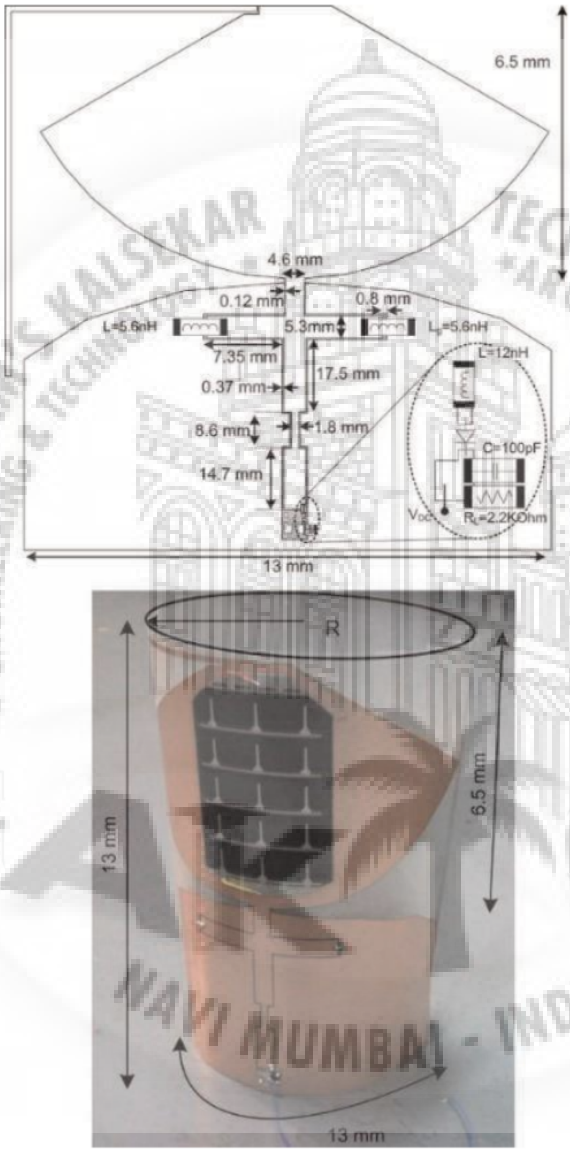

Figure 4.
Hybrid solar/EM rectenna [34].

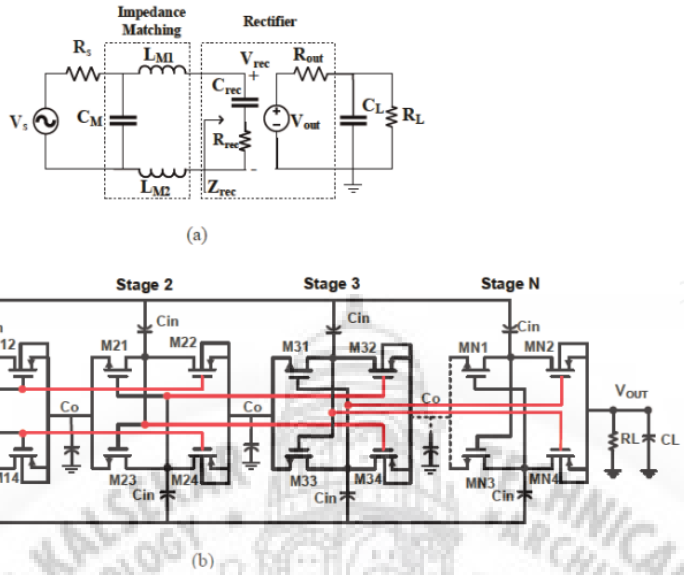

Figure 5.
(a) Proposed RF rectenna equivalent circuit, (b) self-compensated rectifier [35].

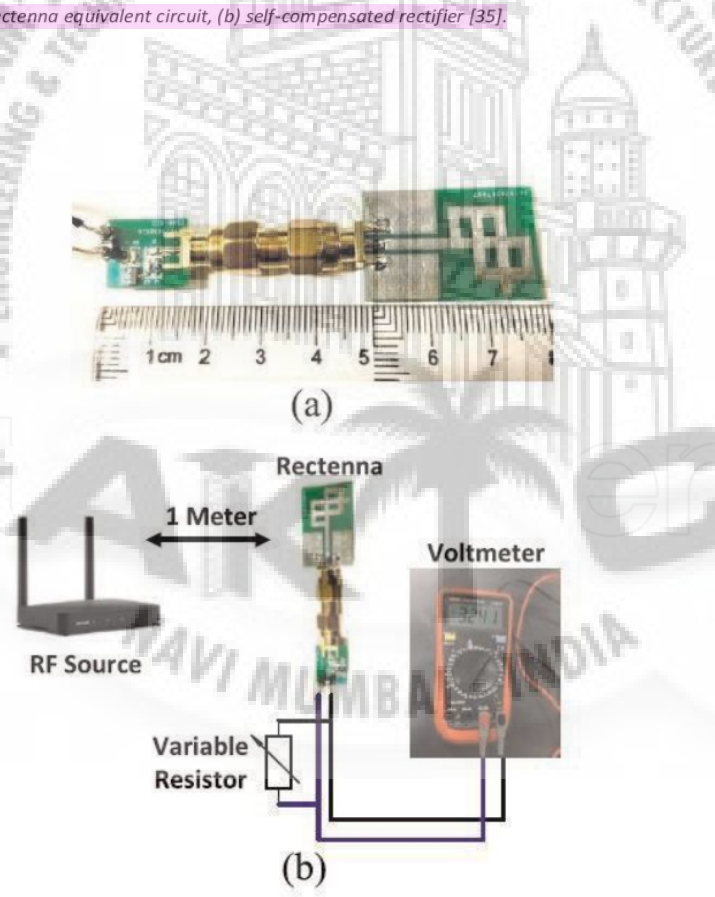

Figure 6.
(a) Complete prototype of the rectenna, (b) measurement set-up for rectenna system [16].

load resistance 0.6KΩ. A compact co-planar waveguide-fed rectenna using a single Cockcroft Walton rectifier platform with the same L-shaped network impedance, shown in Figure 6, is presented in [16]. The efficiency of RF-DC conversion is 68% with the accepted input signal strength of 9 dBm at 6.45 GHz. The rectenna also provides transformation performance of around 43 and 30% at -19 and -22 dBm, respectively.

The next dbm rating is the input rate in the output visewersa

2.2 Single rectenna and multi-band

An easy way to harvest energy harvesting from a single frequency band; this also makes the design of a compatible circuit, which is used to transfer high power between the receiving part of the antenna and the repair circuit, a little easier. In [38], a pentagonal antenna is used with a single-series connecting diode to produce a single band at 7 GHz. The rectenna has a maximum conversion efficiency of 48% at a resistive load of 5 MΩ. At [37], a 3 × 2 rectangular patch array with a gain of 15.6 dBi is used for three stages of Dickson's power harvesting pipeline. The rectenna operates at 915 MHz. Figure 7 shows the antenna list and the repair circuit. The total processing efficiency is 41% at an input power of 10 dBm. A circular antenna with a circular shape was introduced by the X-band planar rectenna (at 3.6 MHz) as shown in Figure 8 [38]. The rectenna provides an effective RF-to-AC conversion efficiency of about 21% for the input power of

156 μW / cm3. A 45 GHz rectenna using a 3 × 4 patch antenna array, shown in Figure 9, is proposed in [39]. The overall efficiency of the RF-to-dc conversion is 45% with an input RF acquired of 15 mW.

Due to the variability in the transmission bands of various wireless systems, there is a large amount of energy wasted at different frequencies. As a result, the

the need for harvest from different groups is growing. In [40], a rectenna is fitted with a triple band. It operates at 406 MHz, 534 MHz and 6.48 GHz with an antenna with integrated and winding design. Figure 10 shows the antenna design in addition to the reconfiguration design. Provides 69% conversion efficiency of 10 dBm input power with 6 MΩ load resistor. The integrated rearrange antenna is introduced on [41] dual band alignment 4.6 and

6.6 GHz. The rated maximum conversion power of the proposed rectenna is 68.5 and 58.9% at 6.20 and 4.6 MHz, respectively, with 16 dBm input power. The type of rectenna formed is shown in Figure 11. The double band rectenna was developed in [42]. Planar converted

The F-antenna is used with a voltage doubler circuit to set up a double band rectenna. The rate is less than 3.6 Khz where the frequnce begins to range its maximum power to vary the frequency of the circuit

By increasing the number of frequencies at which the rectenna can harvest, the weight of the corresponding circuit and the size of the rectenna increases. Therefore,

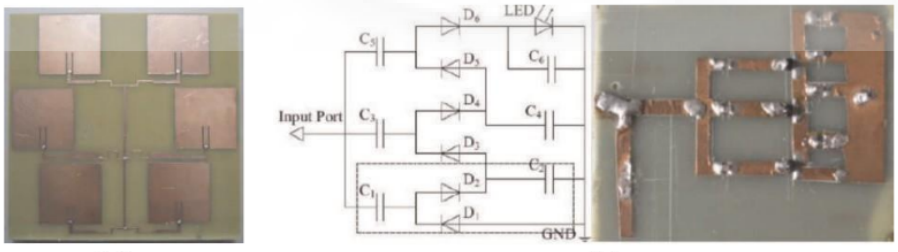

(a) (b)

Figure 7.
Six elements antenna array (a) fabricated patch antenna array, (b) fabricated rectifier [37].

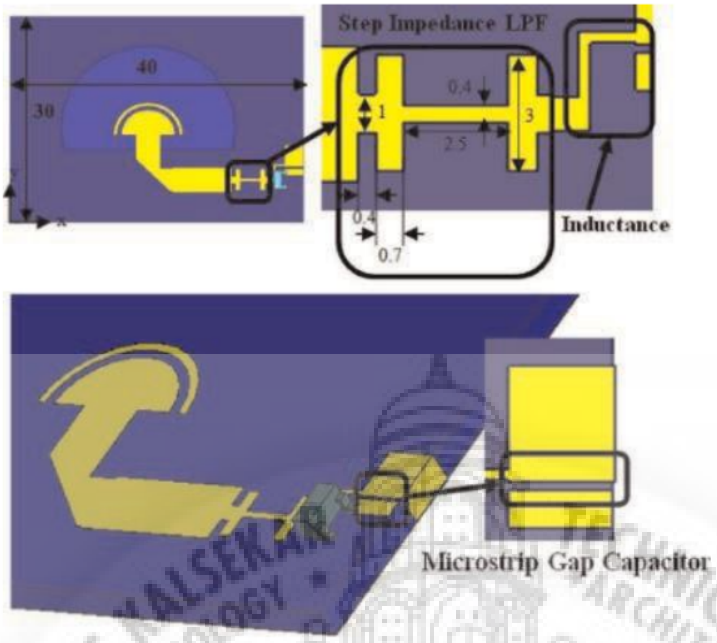

Figure 8.
Geometry of the X-band rectenna [38].

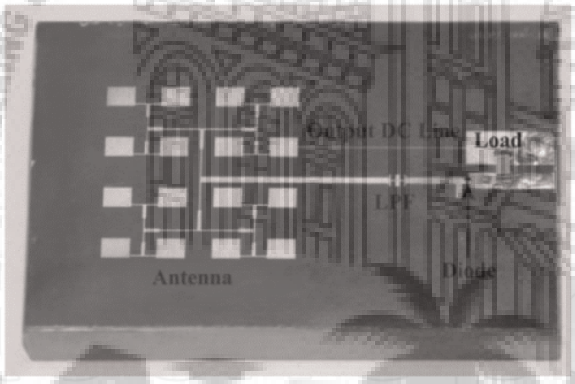

Figure 9.
Fabricated rectenna [39].

The dual-band is the most unique approach to the construction of rectenna systems because it combines between simplicity and fraud from more than one frequency band.

2.3 Extensive installation with electric rectennas

Several studies have been proposed to ensure the more flexible performance of AC-DC over a wider input power band. In [43], a double-band rectifier with a range of input power is suggested. The adjustment and design scheme set is shown in Figure 12. The adjustment provides more than 30% performance with an input range power from 17 to 30 dBm and here

maximum value is 66% from 6 to 16 dBm. Impedance compression network (ICN) techniques is discussed in [44] to fix RF-Ac conversion efficiency over a wide band of input power by maintaining the value of input impedance for the rectifier fixed

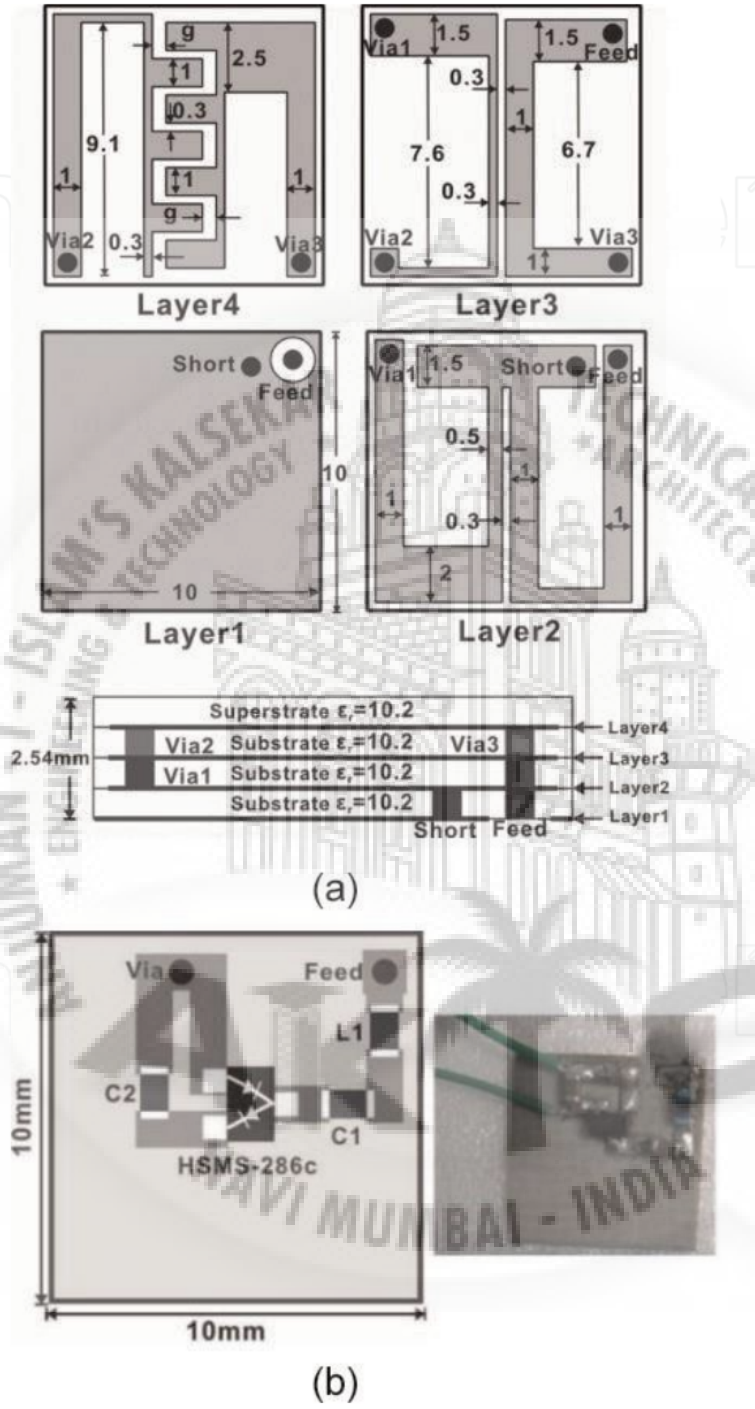

Figure 10.
(a) Triple band antenna, (b) rectifier design and a photo of a fabricated rectifier [40].

Rectenna Systems for RF Energy Harvesting and Wireless Power Transfer
DOI: http://dx.doi.org/10.5772/intechopen.89674

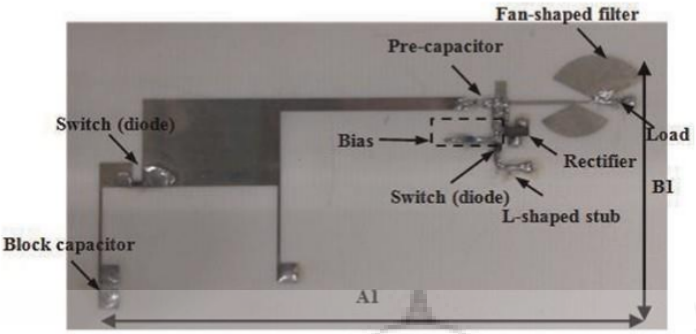

Figure 11.
Fabricated reconfigurable rectenna [41].

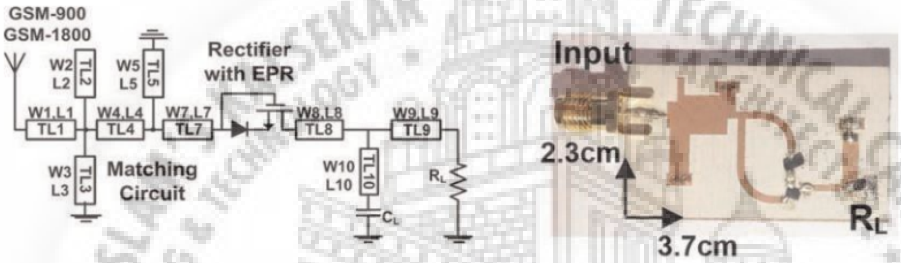

Figure 12.
Schematic diagram and fabricated circuit [43].

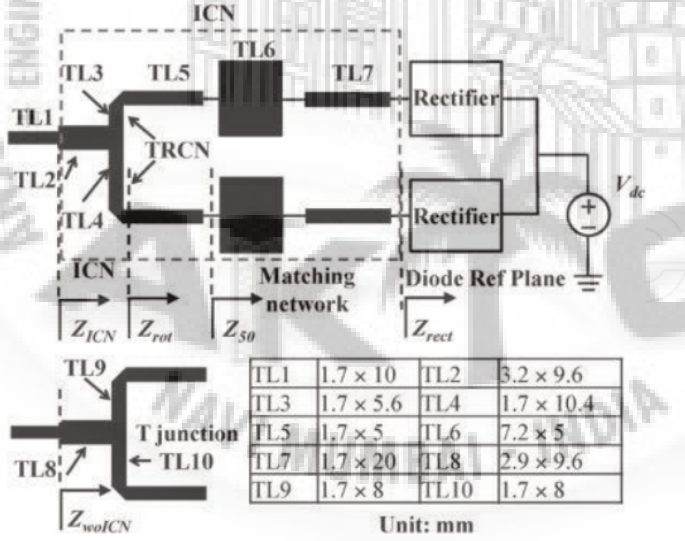

TL1	1.7 × 10	TL2	3.2 × 9.6
TL3	1.7 × 5.6	TL4	1.7 × 10.4
TL5	1.7 × 5	TL6	7.2 × 5
TL7	1.7 × 20	TL8	2.9 × 9.6
TL9	1.7 × 8	TL10	1.7 × 8

Unit: mm

Figure 13.
Layout of the rectifier [44].

regardless of the amount of input power. Figure 13 shows the corrective adjustment. The conditioner has a minimum conversion efficiency of 66% at 45.6 dBm and the input power range of more than 56% is 8.7 dBm

3. Dual-band Retina using voltage double rectifier and four-section matching network

This section introduces a double-band rectenna with a full performance conversion of 65 and 56% at f1 = 2.66 and f2 = 3.6 GHz, respectively, in addition to a wide band of input band, 16 and 14.6 dBm for better performance more than 50% in f1 and f2, respectively. The structure of the stage is as follows: In Section 2.6, a rope construction is introduced. Thereafter, the rotation equivalent to the antenna is discussed in section 3.2. Antenna effects (coefficient coefficient and radiation signals) are discussed in Section 3.3. The simulation network of the dual-team rectifier-antenna is described in section 3.4. The restructuring structure with geometric parameters is shown in section 3.5. The layout of the rectenna test is set in section 3.6. While rectenna configuration incorporates the efficiency of RF-DC conversion over AC power output on both belts discussed in section 3.7.
Dual band rectenna to find a suitable filter for a two-band antenna based on colarization was a design that the antenna suggestion to make a building parameter without CSRR is common. A standard antenna designed for a multi-band.

Construction design

At this stage, an improved antenna design [45] is introduced which will be used to modify the rectenna system. Figure 14 shows the shape of the proposed horn. As shown in the figure, the antenna encloses two layers of substrate (clips 1 and 2). The two layers have the same substrate material with dielectric equilibrium εr1 ¼ εr2 ¼ 4:66, size h1 = h2 = 0.356 mm and a loss tangent of 1.023. The antenna design consists of a disc antenna printed on the top layer of substrate 1. The resonance frequency of this disk is equal to the disc radius as shown in Eq. (1) [46] which may be determined in Eq. (2) [46].

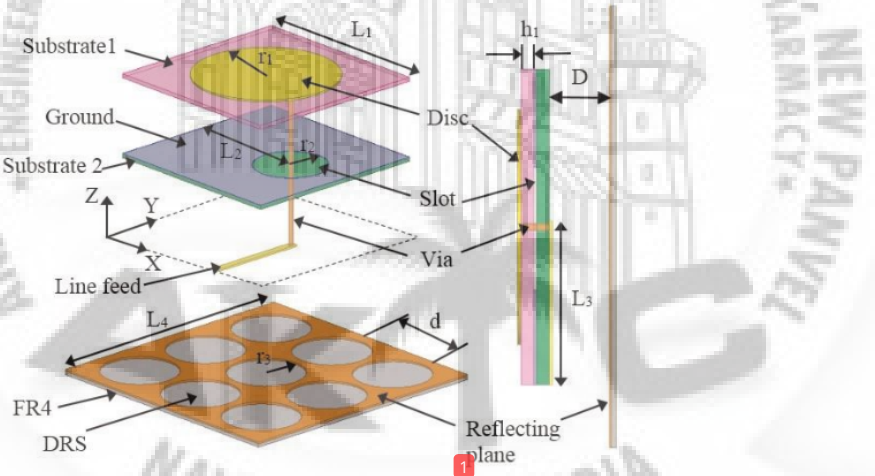

This disk is directly connected to the 56Ω microstrip line using a radio0.6 mm. Also, this disc feeds (by combining) a circular ring in the ground plane between the feed line and the light park, a square plane with a reflector structure (DRS) placed behind the antenna at a distance of λ0 = 6 to improve antenna gain and improve front and back measurement. The display is built on a 0.6 mm thick FR4 substrate with a dielectric thickness of 6.4 and a missing tangent of 0.004. The display is supported by a 15 mm thick layer

Figure 14.
3D geometry, perspective view and side view of the proposed disc antenna [45].

oam with continuous dielectric (εr ¼ 1.36). The size of the substrate is as follows
40 mm × 40 mm. The selected antenna is similar to a person qualified to harvest RF power from mobile radio waves (f2 = 2.63 GHz) and to WLAN wireless communication systems (f1 = 3.48 GHz).

f r ¼ 2πa p ffiffiffiffiffi

(1)

e

Σ 4h.

.πaΣ

ΣΣ0: 6

ae ¼ a 1 þ πaε

ln 2h

þ 1: 696

(2)

3.2 Equilibrium circuit of the proposed antenna (modeling patch antenna)

The first challenge of designing a parallel circuit was to find an accurate model of the proposed antenna in f2 and f3. Figure 15 shows the equivalent circuit used to mimic the antenna power supply in response to an input RF input signal. It is helpful to use this model using the basics R2, L3, and C3, which represent the C1 influence of the first frequency of words (f2), while R3, L1, and C3 represent the second frequency of frequency (f3). Elements L3 and C2 are included in the parallel circuit to represent the electrical length of the feed line and the slot joint, respectively. C2 resistance is similar to the loss of output.
Each radiator (disk and slot) is represented by a connector. Each controller contains a corresponding RLC circuit, the frequency of each weight can be determined from Eq. (3):

1
f r ¼ 2πp ffiffiffiffiffiffiffiffiffi

(3)

First, each resonator is read differently. S-parameters are calculated from the Agilent ADS simulator. After that the resonant and cutoff waves are determined (f0 and fc in GHz, respectively). The initial values of each R and L can be calculated from Eqs. (4) and (5) [47, 48].

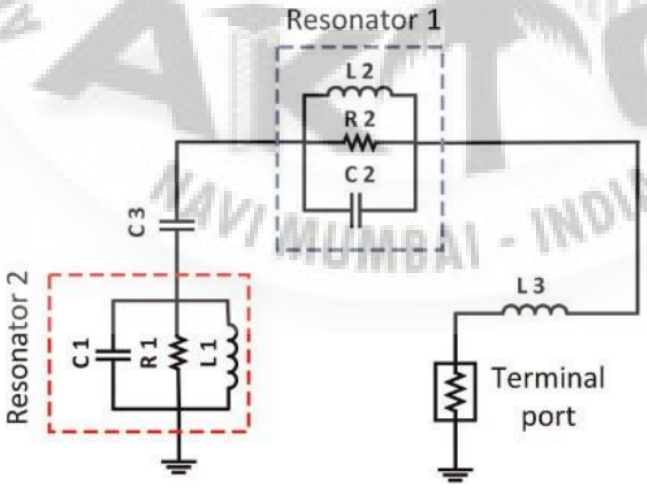

Figure 15.
Equivalent lumped-elements circuit for antenna in ADS

11

Cp ¼

Σ
0 f 0

5 f c
- f

2Σ pF (4)
c

Lp-C

250
Σ
0 f 0

N2 nH (5)

where Cpis capacitance in picofarads and Lpis inductance in nanohenrys.
Table 1 summarizes the initial values of R and L in the two operating frequencies.
Loss resistance can be determined in band factor (Q) -frequency bandwidth (BW) relationships as:

ω0
Q ¼ BW ¼ ω0

RC (6)

f0 no fc C! (C

F 5 fc pF) L! (Lp ¼ 250

2 nH)

π½ f 2 - f 2] Cp ½π f 0]

Resonator 1
(f0 = 2.45 GHz &
= 2.25 GHz)
Resonator 2
(f0 = 1.95 GHz &
fc = 1.65 GHz)

At fc = 2.25 GHz and at f0 = 2.45 GHz, then: Cp = 3.8 pF
At fc = 1.65 GHz and at f0 = 1.95 GHz, then: Cp = 2.4 pF

At f0 = 2.45 GHz and Cp = 3.8 pF, then: Lp = 1.11 nH
At f0 = 1.95 GHz and Cp = 2.4 pF, then: Lp = 2.8 nH

Table 2
Initial L and C values of the two resonators.

Parameter	R1 (Ω)	L1 (nH)	C1 (pF)	R2 (Ω)	L2 (nH)	C2 (pF)	L3 (nH)	C3 (pF)
Number	750	10	1.7	500	1.39	4.15	10	0.2

Table 2.
The material values of the circuit model equal to the dual band antenna.

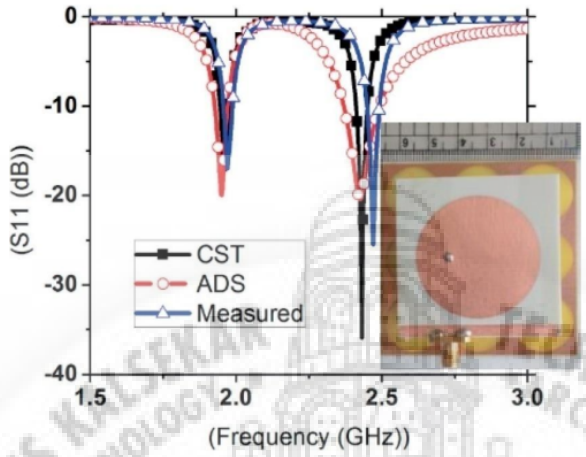

Figure 16.
Reflection coefficient of the proposed antenna.

when the frequency bandwidth of electrical energy is tested from Eq. (7).

1
BW ¼ RC (7)
Thereafter, the resistance loss (R) of each resonator can be determined as:

1
R, BW × C (8)
After combining the two resonators, taking into account the loss-resistant effect (R1 and R2) in addition to efficiency, a similar final circuit can be obtained. The corresponding values of the regional equities are shown in Table 2.

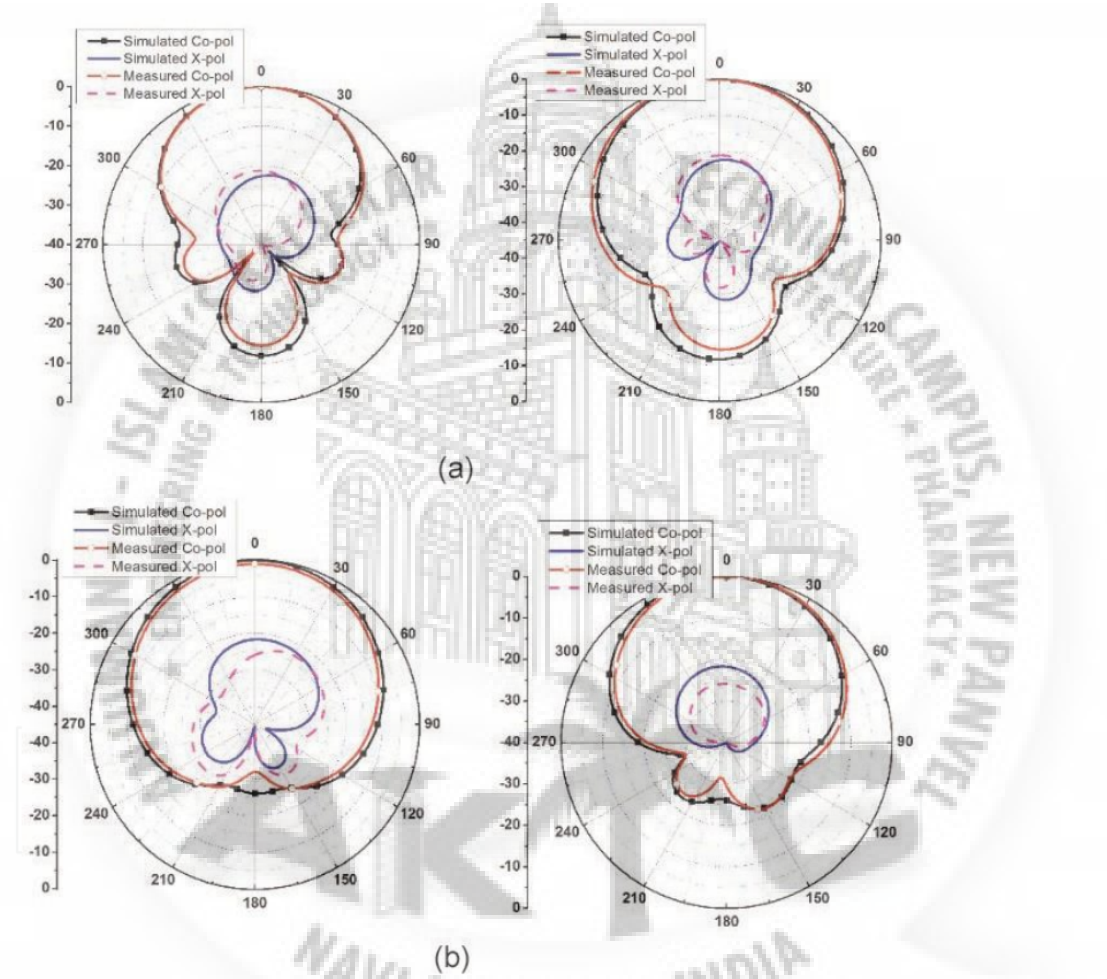

Figure 17.
2D measured and simulated results of radiation pattern for the antenna: (a) at 1.95 GHz and (b) at 2.45 GHz.

Antenna measurement results

Designed antenna S-parameters

Figure 16 shows the proportional response of the antenna obtained in the CST simulation compared to the calculated response of the equivalent circuit model using the Agilent ADS software in addition to the indicated coefficient of display. Good agreement was between the results of the standardized, rated environment and ADS. The antenna sounds in both 4.95 GHz (f1) and 4.25 GHz (f2) bands. The circular band is designed to output at 5.65 MHz with direct feed and transmission line placed behind substrate 2. While, the resonance of 2.56 GHz is designed to output due to the strong interaction between the rounded surface above substrate 1 and the circular area found on the ground plane, at 6.5 GHz the disc antenna is considered to be a circular space supplier. The operation of the proposed antenna was developed and modified by commercial EM software CST Microwave Studio. An example of the proposed antenna was developed and tested. The display dimensions of the antenna are rated by R&S ZVA 67 Network Analyzer. It is well known that the resulting and measured results of the antenna input parameters are well consistent.
Only, a slight change in the estimated S parameters was observed due to the connection of the connector, false tolerance, adhesion between the two antenna layers and the alignment of the layers in the process.

Radiation characteristics

The resulting and measured effects of the E and H-plane antenna for high gain in f1 and f2 are shown in

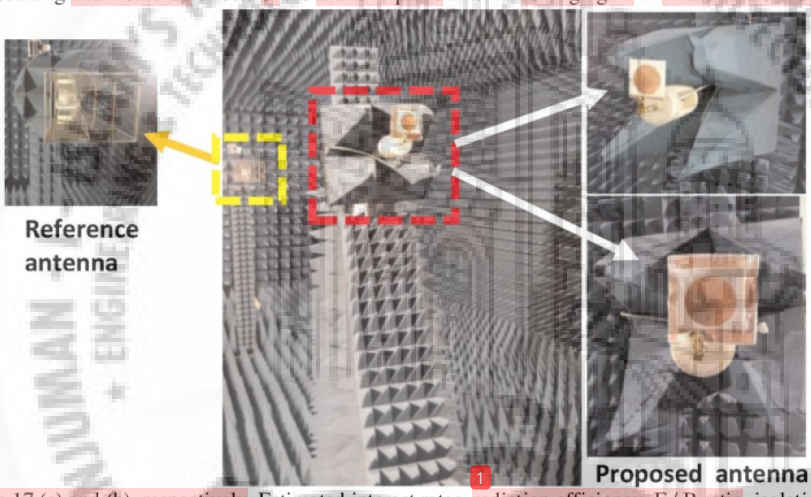

Figure 17 (a) and (b), respectively. Estimated interest rates, radiation efficiency, F / B ratio, isolation level, 3 dB beamwidth round on the first resonance frequency (f1) is 9.6 dBi, 40%, 14, 25.5 dB, 52.5 °, respectively . While in the second resonance frequency, these values can be summarized as 8.4 dBi, 5.6%, 35, -41.6 dB, 56.2, respectively. The gain and radiation pattern of the antenna is measured by the Anechoic Chamber shown in

Figure 18.
Antenna radiation pattern measurement set-up.

Figure 18. There is a good agreement between the simulated and measured results of the radiation characteristics.

Rectifier-antenna matching

In this project, a system used in [49] was implemented to achieve a dual-band imped- ance change in two frequency groups (f1 and f2). This system is used to compare between the impedance intake of the complex and highly dependent rectifier (and the actual impedance of the antenna (ZAnt) through four different phases (Section 1-4) as shown in Figure 19. summarized the following steps:
Step 1: Obtain a correlation between the loading values both used waves, i.e., to move the load impedance values (the rectifier) into Smith's chart to be placed in a real circle with the assumed parts equal to both sides of Smith's chart as shown in Figure 20.
Step 2: Cancel the assumed portion of the impedances in f1 and f2.
Step 3: Real to real impedance change.

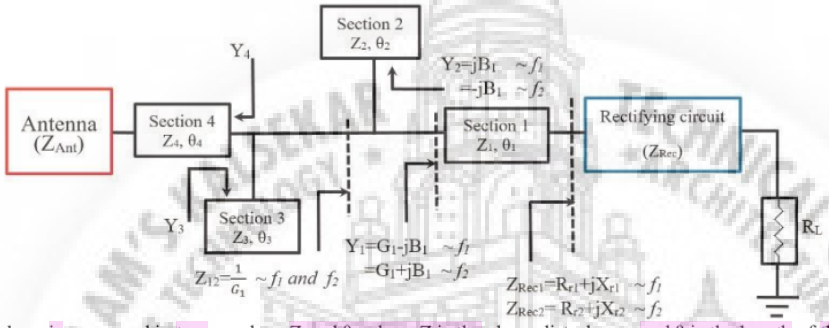

Each phase is expressed in two numbers Z and θ, where Z is the phase disturbance and θ is the length of the electric phase. The task of the first phase (Phase 1) is to make the actual value of the input impedance of the correction in

Figure 19.
Dual-band matching circuit.

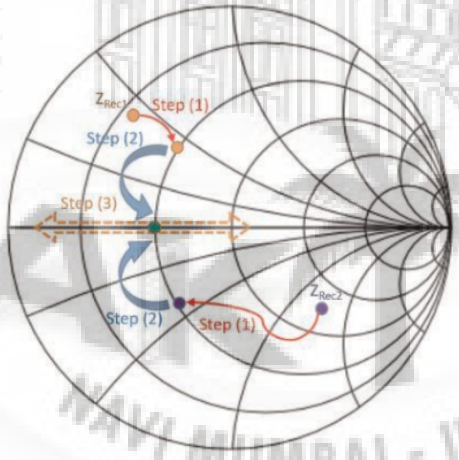

Figure 20.
Matching steps indicated on smith chart.

f1 is equal to that of rectifier impedance input to f2 and the components considered are also equal but have opposing signals (one is bright (provocative reaction) and the other is negative (capacitive reactance)); Phase 1 parameters (Z1 and θ1) can be calculated from [50] as:
s. ffiffiffi Σ ffiffiffi

Z ¼ R R

X X X

þ Xr1, Xr2, X

- R X Þ

(9)

1 r1 r2

r1 r2

Rr2 - Rr1

r1 r2

r2 r1

¼1 ¼

and arctan Z1 ðRr1 —Rr2 Þ
Rr1 Xr2 —Rr2 Xr1

þm þ 1Þ

(10)

where n is the wrong number and m = f2 / f1. Section 2 is used to cancel the hypothetical components of the introduction of Y1 at two frequencies f1 and f2. The boundaries of section 2 can be determined as [49]:

color θ2
Z2
B1

(11)

θ ð1 þ pÞπ
ð1 þ mÞ

(12)

where p is a whole number. Sections 3 and 4 are used for real impedance conversion, and their parameters can be calculated from Eqs. (13) - (17) [49, 51]
s ffi.ffiffiffiffiffiffiffiffiffiffiffiffiffiffiffiffiffiffiffiffiffiffiffiffiffiffiffiffiffiffiffiffiffiffiffiffiffiffiffiffiffiffiffiffiffiffiffiffiffiffiffiffiffiffiffiffiffiffiffiffiffiffiffiffiffiffiffiffiffiffiffiffiffiffiffiffiffiffiffiffi
Σ ffiffiffiffiffiffiffiffiffiffiffiffiffiffiffiffiffiffiffiffiffiffiffiffiffiffiffiffi

Z4 ¼

ZAntð1 þ tan 2θ4Þ

G1

- ZAnt

1

color θ4

(13)

ð ð 1 þ sÞπ
ð1 þ mÞ

(14)

color θ3
Z3
B4

(15)

ð ¼ ð 1 þ qÞπ

(16)

. ð1 þ mÞ
Z - Z tan θ

B ¼ The ant 4

(17)

4 2
The ant

× Z4

þ Z3 × tan 2θ4

where q and s are numbers

Repair design

Multiple rectifiers topologies are used for power harvesting, for example, diodes for parallel connections, diodes for series connections, double voltage circuits, multi-voltage power supply and so on. Voltage multipliers produce high loads from a low voltage power source. However, in this design a double power circuit, which is a special case of electric power multipliers, is used for adjustment to obtain high power with easy design maintenance. The design of the fix and the same network are shown in Figure 21 [52]. The double voltage circuit consists of two Avago HSMS2655 Schottky diodes and two SMD capacitors (Cs = Cp = 156 MF). Scottky diode has a built-in voltage (Vb) for
0.150 V and a voltage breakdown (Vbr) of 5.4 V. Due to the small series resistance and blocking forces (Rs of 36Ω and Cb of 15.25 þF) for the

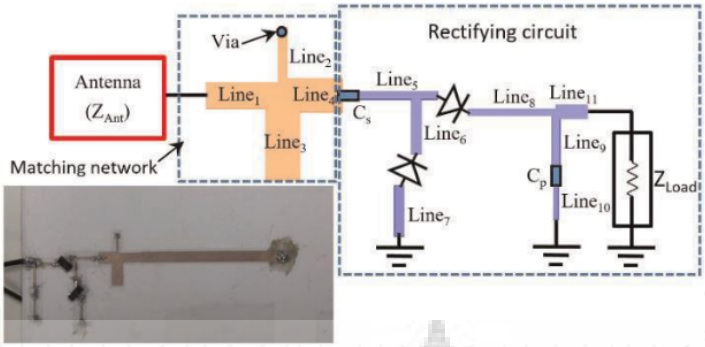

Figure 21.
Corrective structure; L1 = 4.5 mm, W1 = 1.54 mm, L2 = 4 mm, W2 = 0.33 mm, L3 = 5 mm, W3 = 1.96 mm, L4 = 3.52 mm, W4 = 2 mm, L5 = 4 mm, W5 = 0.36 mm, I-L6 = 4.98 mm, W6 = 0.31 mm, L7 = 5 mm, W7 = 0.29 mm, L8 = 5.1 mm, W8 = 0.43 mm, L9 = 4.8 mm, W9 = 0.3 mm, L10 = 4.88 mm, W10 = 0.33 mm, L11 = 1.81 mm, W11 = 0.84 mm.

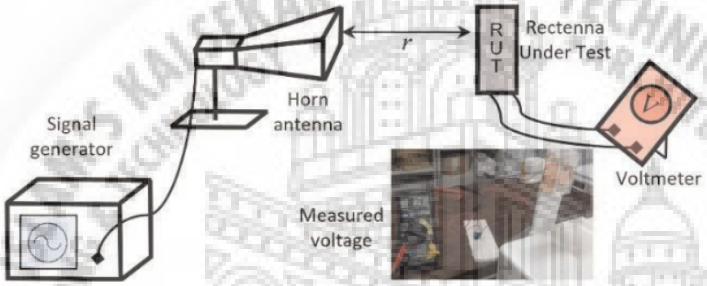

Figure 22.
Rectenna measurement setup.

the category of diodes mentioned above, so these diodes have a high frequency of cutting and efficiency of conversion. Capacitors Cs are used to store power in one half cycle to double the charging power of Cp in another half cycle, Cs also act as a bandpass filter to block DC power from wireless diodes. Cp has two functions, which are used to bypass high-speed modes, produced from a non-grounded diode and to obtain a smooth DC output voltage. And the shunt connection between Cp and RED impedance RL acts as a low pass filter.

The modifier is designed for Rogers Duroid RO3003 with 3 ()r) relative to it, substrate size (h) of 0.76 mm, dielectric loss tangent (tanδ) of 0.0013 and copper (t) thickness of 0.017 mm. The complex impedance of the compl1.ex input (ZRec) at the two frequencies is (8 —j × 28.2) and (26.1 —j × 39.7) in f1 and f2, respectively, with a positive load of 1.5 kΩ. Regional parameters are designed to achieve maximum conversion efficiency in two bands of frequency input power levels obtained. The adjustment parameters and the corresponding circuit are shown in Figure 21, where each line is defined by length (L) and width (W). Also, the type of adjustment made is shown in Figure 2

Rectenna measurements

The rectifying circuit including the matching network is simulated using Keysight advanced design system (ADS), while the antenna was designed usin

ANSYS high-frequency structure simulator (HFSS). The advanced gain gain antenna described in [45] is used as a gain antenna in the proposed rectenna to increase the sensitivity of the fixer. Therefore, increasing the rectenna capacity of the harvester from lower input power levels. The receiving antenna and the amplifier are integrated into the

same substrate, built and measured in the measurement setting shown in Figure 22. Agilent Technologies E8257D Analog signal is used to transmit a microwave signal connected to a two-dBi horn antenna with two gain frequencies. On the other hand, a rectangle under test (RUT) is connected to a voltmeter to measure DC power. To monitor the performance of the antenna radiation, the effective antenna area is considered. Therefore, the efficiency of the RF-DC conversion of the proposed rectenna (η) is calculated as follows:

2
η DC 100 (18)
Phina × RL
where the VDC is the rated DC output power, the Pin is the input power of the RF received and the RL is the resistance load. The pin is described in Eq. (19)

Pin ¼ PD × Aeff (19)
where PD is the RF power source and Aeff is the active antenna. PD and Aeff are calculated using Eqs. (20) and (21), respectively.

PtGt PD-4πr2
λ2

(20)

Aeff-Gr 4π (21)
Pt with transmitting power, Gt is the horn antenna advantage and r distance between the transmitter and rectenna are all known. Therefore, the efficiency of RF-to-DC conversion can be measured. For remote field measurements, r is selected 40 cm. Figure 23 shows a picture of the rectenna scale setting.

Rectenna results and interview

The whole system (antenna, compatible circuit and amplifier) has been tested in addition to

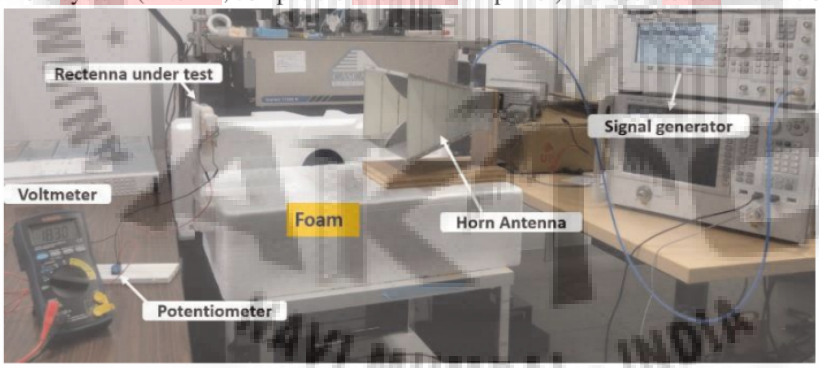

different input rates for different load loads in two waves

Figure 23.
Photo of the measurement setup

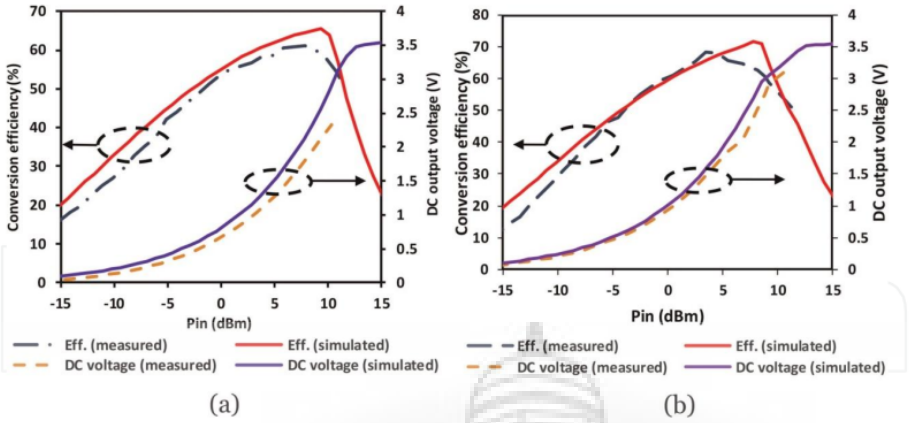

Figure 24.
Simulated and measured conversion efficiency in addition to the DC output voltage versus input power (a) at f_1 (b) at f_2.

(f1 no f2); Figure 24 (a) and (b) show a comparison between the estimated and actual effects of RF-to-DC efficiency and DC output power compared to the input power f1 and f2, respectively. The average conversion efficiency is 63% with an input power of 14 dBm (from - 2.6 to 15.5 dBm) in f1, while the average efficiency in f2 is 66% with an input power from -6.5 to 51 dBm (12.3 dBm). There is a slight variation between the measurement and measurement results, where the efficiency of AC-DC conversion is 56 and 63% in two similar frequencies, respectively. Due to limitations in testing, the input power received is limited to 25 dBm.

Chapter 4

4. Conclusions

This chapter presents a study of rectenna systems for RF energy harvesting and power transmission. Research is being done on the recruitment of rectennas in WPT, low-cost inputs for electric rectennas, single and multi-band rectennas, wide-ranging inputs for electric rectennas are being introduced. Finally, a double-band rectenna is used using a voltage doubler rectifier and a network corresponding to four phases. The first part of the rectenna design is a dual-band disc antenna with the advantage of being designed to collect high RF power. It output at 2.65 and 5.46 GHz. The estimated results showed a gain of 7.39 and 6.87 dBi at 2.63 and 5.66 GHz, respectively.

The disc antenna is integrated with a double-band rectifier with four components of the same network to introduce a double-frequency rectenna with high conversion performance over a multiband RF power output band. The rectenna provides high efficiency of AC-DC rated conversion of 56% and 70% at 3.56 GHz and 4.5 GHz, respectively. and works beyond the scope of the input power; includes a range of 16 and 16.3 dBm in f1 and f2, respectively for higher conversion efficiency above 55% with load resistance (RL) = 1.2K. The rectenna was designed, built and measured. The results produced and measured show good agreement.

References

[1] Kim D, Park J, Park HH, Ahn S. The production of magnetic force and the torque of a microrobot using a power transmission coil. EEE transactions in Magnetics. 2015; 51 (11): 1-4

[2] Ahn D, Kim SM, Kim SW, Moon J, Cho IK. Wireless power transmission receiver with coil equipment is widely accepted. IEEE transactions in Industrial Electronics. 2018; 66 (5): 4003-4012

[3] Kim T, Yun G, Lee WY, Yook J. Asymmetric coil are the structures of the most efficient electrical transmission systems. IEEE transactions in Microwave Theory and Techniques. 2018; 66 (7): 3443-3451

[4] Hekal S, Abdel-Rahman AB, Jia H, Allam A, Pokharel RK, Kanaya H. Strong resonant coupling for short-range wireless transfer applications using a defected ground structures. To: IEEE Conference Power Transfer Transfer (WPTC),
Colorado, USA. 2015

[5] Hekal S, Abdel-Rahman AB, Jia H, Allam A, Barakat A, Pokharel RK. The novel process of wireless power transmission systems using built-in structures. IEEE transactions in Microwave Theory and Techniques. 2017; 65 (2): 591-599

[6] Tahar F, Barakat A, Saad R, Yoshitomi K, Pokharel RK. Dual-band dual structures that disable the power transmission system through external coupling and interon resonator. IEEE transactions in Circuits and System II: Express Briefs. 2017; 64 (12): 1372-1376

[7] Sasaki S, Tanaka K, Maki K. Microwave energy transfer

solar energy satellite technology. IEEE procedures. 2013; 101 (6): 1438-1447

[8] McSpadden P, Jaffe J. Energy modification and transfer of solar energy space modules. IEEE procedures. 2013; 101 (6): 1424-1437

[9] Li X, Duan B, Song L, Zhang Y,
Xu W. Study of treadped amplitude distribution taper for microwave power transmission for SSPS. IEEE transactions on antennas and distribution. 2017; 65 (10): 5396-5405

[10] Nguyen VT, Kang SH, Choi JH, Jung CW. Powerful power transmission system uses a three-coil system with a single planet receiver for laptop applications. IEEE transactions in Consumer Electronics. 2015; 61 (2):
160-166

[11] Lower ZN, Chinga RA, Tseng R, Lin J. Design and wireless power transmission system testing. IEEE transactions in Industrial Electronics. 2009; 56 (5): 1801-1812

[12] Wireless charging pad, Black Sapphire. Samsung Mobile, Samsung Electronics America. [Online]. Available at: http://www.samsung.com/us/ mobile / cell-phones-accessories / eppg 920ibugus

[13] Wang G, Liu W, Sivaprakasam M, Kendir GA. Composition and analysis of dynamic electrical telemetry of biomedical biomarkers. IEEE Transactions in Circuits and Programs I: General Papers. 2005; 52 (10): 2109-2117

[14] Jou AY, Azadegan R, Mohammadi S. High resistance to CMOS SOI rectenna for uninstalled applications. Books for IEEE Microwave and Wireless Components. 2017; 27 (9): 854

Project report

ORIGINALITY REPORT

61%	60%	52%	6%
SIMILARITY INDEX	INTERNET SOURCES	PUBLICATIONS	STUDENT PAPERS

PRIMARY SOURCES

1	www.intechopen.com Internet Source	31%
2	mts.intechopen.com Internet Source	20%
3	Submitted to Indian Institute of Technology, Bombay Student Paper	2%
4	www.slideshare.net Internet Source	2%
5	Mohamed Aboualalaa, Hala Elsadek. "Chapter 8 Rectenna Systems for RF Energy Harvesting and Wireless Power Transfer", IntechOpen, 2020 Publication	2%
6	Mohamed Aboualalaa, Islam Mansour, Adel B. Abdelrahman, Ahmed Allam, Mohamed Abo-zahhad, Hala Elsadek, Ramesh K. Pokharel. "Dual-band CPW rectenna for low input power energy harvesting applications", IET Circuits, Devices & Systems, 2020 Publication	1%

7	www.aiktcdspace.org:8080 Internet Source	1 %
8	pdfs.semanticscholar.org Internet Source	1 %
9	Mohamed Aboualalaa, Islam Mansour, Mohamed Mansour, Adel Bedair et al. "Dual-band Rectenna Using Voltage Doubler Rectifier and Four-Section Matching Network", 2018 IEEE Wireless Power Transfer Conference (WPTC), 2018 Publication	1 %
10	docplayer.net Internet Source	<1 %
11	www.coursehero.com Internet Source	<1 %
12	hdl.handle.net Internet Source	<1 %
13	Gopinath Samanta, Debasis Mitra, Sekhar Ranjan Bhadra Chaudhuri. "Miniaturization of a patch antenna using circular reactive impedance substrate", International Journal of RF and Microwave Computer-Aided Engineering, 2017 Publication	<1 %

Exclude quotes	Off	Exclude matches	Off
Exclude bibliography	Off		